# KEH-Gait: Using Kinetic Energy Harvesting for Gait-based User Authentication Systems

Weitao Xu, *Member, IEEE*, Guohao Lan, Qi Lin, Sara Khalifa, *Member, IEEE*, Mahbub Hassan, Neil Bergmann, and Wen Hu, *Senior Member, IEEE*

**Abstract**—With the rapid development of sensor networks and embedded computing technologies, miniaturized wearable healthcare monitoring devices have become practically feasible. For many of these devices, accelerometer-based user authentication systems by gait analysis are becoming a hot research topic. However, a major bottleneck of such system is it requires continuous sampling of accelerometer, which reduces battery life of wearable sensors. In this paper, we present *KEH-Gait*, which advocates use of output voltage signal from kinetic energy harvester (KEH) as the source for gait recognition. *KEH-Gait* is motivated by the prospect of significant power saving by not having to sample the accelerometer at all. Indeed, our measurements show that, compared to conventional accelerometer-based gait detection, *KEH-Gait* can reduce energy consumption by 82.15 percent. The feasibility of *KEH-Gait* is based on the fact that human gait has distinctive movement patterns for different individuals, which is expected to leave distinctive patterns for KEH as well. We evaluate the performance of *KEH-Gait* using two different types of KEH hardware on a data set of 20 subjects. Our experiments demonstrate that, although *KEH-Gait* yields slightly lower accuracy than accelerometer-based gait detection when single step is used, the accuracy problem can be overcome by the proposed Probability-based Multi-Step Sparse Representation Classification (PMSSRC). Moreover, the security analysis shows that the EER of KEH-Gait against an active spoofing attacker is 11.2 and 14.1 percent using two different types of KEH hardware, respectively.

**Index Terms**—Authentication, gait recognition, energy harvesting, wearable devices, sparse representation

## 1 Introduction

Wearable health-monitoring systems have received a great deal of attention from both the industry and the research community in the last decade. It is predicted that by 2025, the market for personal wearable devices will reach 70 billion dollar. The major deployments of those devices are expected to be in health monitoring and medical assistance domains [1], [2], [3]. Some popular wearable devices, such as Fitbit and Apple Watch, are already monitoring and storing a mass of sensitive health data about the user. The private information of users can be further explored to provide a variety of emerging applications in the healthcare area. For example, the collected sensory data can be explored for the understanding of user's physical and mental health states [4], [5].


- *W. Xu is with the College of Computer Science and Software Engineering, Shenzhen University, Shenzhen, Guangdong 518060, China. E-mail: weitao.xu@szu.edu.cn.*
- *G. Lan, Q. Lin, M. Hassan, and W. Hu are with the School of Computer Science and Engineering, University of New South Wales, Sydney, NSW 2052, Australia. E-mail: {glan, mahbub, wenh}@cse.unsw.edu.au, qi.lin@student.unsw.edu.au.*
- *S. Khalifa is with the Distributed Sensing Systems Research Group, Data61, CSIRO, Eveleigh, NSW 2015, Australia. E-mail: sara.khalifa@data61.csiro.au.*
- *N. Bergmann is with the School of Information Technology and Electrical Engineering, University of Queensland, St Lucia QLD 4072, Australia. E-mail: n.bergmann@itee.uq.edu.au.*


*Manuscript received 1 May 2017; revised 5 Mar. 2018; accepted 10 Apr. 2018. Date of publication 20 Apr. 2018; date of current version 3 Dec. 2018. (Corresponding author: Guohao Lan.)*
*For information on obtaining reprints of this article, please send e-mail to: reprints@ieee.org, and reference the Digital Object Identifier below.*
*Digital Object Identifier no. 10.1109/TMC.2018.2828816*

However, such wearable systems are vulnerable to impersonation attacks in which an adversary can easily distribute his device to other users so that data collected from these users can be claimed to be his own. In this way, the attacker can claim potential healthcare profits that are allocated to people with certain illnesses even though he may not have any illnesses [6]. For instance, a policy holder may obtain a fraudulent insurance discount from a healthcare insurance company by using other people's health data. Another example is that in a mobile healthcare system for disease propagation control [7], an attacker can obtain additional vaccine allocation by launching user impersonation attacks and thus compromise the regular operations of such systems.

To mitigate the risk of malicious attacks, most wearable devices rely on explicit manual entry of a secret PIN number. However, due to the small screens of wearable devices and frequent unlocking requests, it is inconvenient for users to enter the keys manually. Furthermore, this method is not applicable when an adversary colludes with other users to spoof the healthcare company.

Gait recognition using wearable sensors, such as accelerometers, has emerged as one of the most promising solutions for user authentication. Extensive previous studies have already demonstrated its feasibility in user authentication [8], [9], [10], but they have also shown that continuous accelerometer sampling drains the battery quickly. High power consumption of accelerometer sampling, which is typically in the order of a few milliwatts, also makes it challenging to adopt gait-based user authentication in resource-constrained wearables. Although power consumption may be not a big issue for wearables with large batteries such as smartphone, other wearables like Implantable Medical

Devices (IMDs) suffer from short battery life because IMDs are long-lived devices and battery replacement requires surgical intervention [11].

A vision for wearable devices is to be battery-free (self-powered). A current trend in battery-free devices is to investigate kinetic energy harvesting (KEH) solutions to power the wearable devices [12], [13], [14], [15]. However, one fundamental problem in KEH is that the amount of power that can be practically harvested from human motions is insufficient to meet the power requirement of accelerometer for accurate activity recognition [16]. As reported in [12], the amount of power that can be harvested from human motion is only in the order of tens to hundreds of microwatts. They also report that assuming 100 percent conversion efficiency, the power can be harvested from walking is only 155 $\mu W$. This 2-3 orders of magnitude gap between power consumption and power harvesting is the biggest obstacle for realising gait-based authentication in batteryless wearables. Although the power consumption of sensors has been largely reduced in the last years thanks to the Ultra-Low-Power electronics [17], we believe in the near future energy harvesting will be used to augment or substitute batteries. For example, AMPY [18] has released the world's first wearable motion-charger which can transform the kinetic energy from user's motion into battery power. SOLEPOWER [19] produces smart boots that use user's steps to power embedded lights, sensors and GPS.

Motivated by this prospect, we propose gait recognition by simply observing the output voltages of KEH. The feasibility of the proposed idea is based on the observation that if humans have unique walking patterns, then the corresponding patterns of harvested power from KEH should be unique too. The proposed system offers several advantages. The major advantage of KEH-based gait recognition is the potential for significant power savings arising from not sampling accelerometer at all. On the other hand, the output voltage can be used to charge the battery, thus further extending battery life. Finally, as energy harvester will be integrated in wearable devices in the near future, the output voltage can be naturally utilized for authentication purpose without introducing extra sensors. This makes it a promising solution for light-weight authentication for wearable devices. The main challenge of implementing such a system is achieving high recognition accuracy by using a 1-axis voltage signal rather than 3-axis accelerometer signals. We address this issue by proposing a novel probability based sparse fusion method which exploits the information from multiple steps. The main contributions of this paper are as follows:

- We propose a novel gait-based user authentication system for mobile healthcare system, called KEH-Gait, which uses only KEH voltage as the source signal to achieve user authentication.
- We build two different KEH prototypes, one based on piezoelectric energy harvester (PEH) and the other on electromagnetic energy harvester (EEH). Using these KEH devices, we evaluate gait recognition accuracy of KEH-Gait over 20 subjects. Our results show that, with conventional classification techniques, which operate over single step, KEH-Gait achieves approximately 6 percent lower accuracy compared to accelerometer-based gait recognition.
- We demonstrate that authentication accuracy of KEH-Gait can be increased to that of accelerometer-based gait detection by employing a novel classification method, called Probability-based Multi-Step Sparse Representation Classification (PMSSRC), which efficiently fuses information from multiple steps.
- Finally, using measurements, we demonstrate that currently available microprocessors can read KEH voltage within 33 $\mu s$, which is two orders of magnitude faster than what it takes to wakeup, interrogate and read acceleration values from typical 3-axis accelerometers. This means that with microprocessor duty cycling, KEH-Gait promises major energy savings over conventional accelerometer-based gait detection.

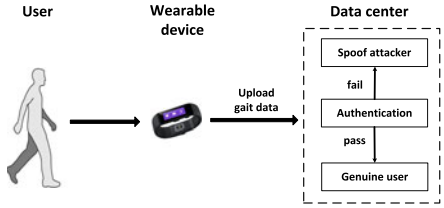


Fig. 1. Overview of a typical healthcare monitoring system.

This paper is an extension of our previous work [20]. Compared to the previous conference paper, there are three aspects of improvement. First, we apply SVD-based noise reduction method to reduce the impact of noise in signal processing phase (Section 3.2.1). Then, we employ dictionary learning technique (Section 3.3.2) and column reduction approach (Section 3.3.3) to build more advanced training model. Finally, we propose a novel probability-based classification approach in classification phase to further improve classification accuracy (Section 3.4). Building on the strengths of these approaches, we find that the accuracy is improved by 3-5 percent and the energy saving is improved from 78.15 to 82.15 percent.

The rest of the paper is structured as follows. Section 2 introduces trust models and attacker models of gait-based authentication system. Section 3 presents the system architecture of KEH-Gait. Prototyping of KEH wearables and gait data collection are described in Section 4. We present evaluation results in Section 5, and analyze power consumption in Section 6. We introduce related work in Section 8 before concluding the paper in Section 9.

## 2 Trust and Attack Models

We envision the use of KEH-Gait primarily in resource-constrained healthcare monitoring wearable devices to authenticate the identity of the user to prevent spoof attack. KEH-Gait addresses the issue of short battery life by using an energy harvester to replace an accelerometer. In the near future, energy harvesters can even be integrated in the hardware system to achieve battery-free wearable devices. Fig. 1 illustrates the workflow of a typical healthcare monitoring system. In such a system, each user is given a unique user ID and a monitoring application which runs on a wearable device that can collect private sensor data and transmit them to the data centre of a healthcare company. Before transmission, the device first collects gait data and transmits them to the sever. The server will then perform authentication to verify the user's identity by using the gait data. If the user passes authentication, the further private data like blood pressure or heart rate are then transmitted to the server. While if the user verification fails, i.e., the user spoofing attack is detected, the sensor data collected from this user's device will not be reported to the server. In the server,

sensor data will be analysed and processed by the healthcare company to derive user's physical and mental conditions. For instance, the measurements of heartbeats and blood pressure can be used to predict user's psychological conditions. A wide range of applications can also be enabled by such mobile healthcare systems and some examples are:

- User's physical behaviors are often reflection of physical and mental health and can be used by healthcare companies to facilitate early prediction of future health problems like depression [4].
- Health food companies can make advertisement by cooperating with healthcare related applications such as "IDOMOVE"[1], e.g., providing discount coupons for users who walk more than 1hr a day.

### 2.1 Trust Model

In this paper, we assume the data collected by sensors built in the wearable devices are trustworthy. Also, our system trusts the communication channel between the wearable device and the healthcare company's server. We discuss the feasibility of our assumption as follows.

*Tamper-Resistant Sensor.* An attack can physically accesses to the sensor or chipset and manipulate the recorded data. To make sure the device has not been modified, a healthcare company can apply tamper-resistant techniques [21]. As mentioned in [22], ARM TrustZone extension can also be used to ensure the integrity of the sensors [23].

*Trusted Transmission.* A man-in-the-middle(MITM) attack may occur when the device is communicating with the server. Therefore, the device and server should establish a secure communication channel. To address this attack, the healthcare company can install a digital certificate in the wearable device and the device will perform Secure Sockets Layer (SSL) authentication when communicating with the server.

*Security Against Malicious Operator.* Although gait data are collected in KEH-Gait, they are not stored and transmitted in cleartext. As will be discussed in Section 3, we apply a projection matrix (compressed matrix) $R_{opt}$ on original signal to obtain the compressed samples. Without the knowledge of $R_{opt}$, a malicious operator cannot recover the original gait signal according to compressive sensing theory [24]. Apart from our method, an alternative approach is presented in a similar work which uses fuzzy commitment scheme to maintain the security of gait template [25]. Another potential problem is one user may own several wearable devices while he/she has a unique gait only. This problem can be addressed by using different projection matrices for different devices.

### 2.2 Attack Model

The aforementioned mobile healthcare system is vulnerable to user spoofing attacks. For instance, an adversary can distribute his device to another person, and upload the data of that person aiming to obtain healthcare benefits. Besides, multiple users may collude to launch user spoofing attacks to fool the mobile healthcare system. Therefore, the adversary model considered in this paper focuses on impersonation attacks. We assume the presence of two types of impersonation attacks:

- A passive adversary. The passive adversary tries to spoof the healthcare system by using his own walking patterns.
- An active adversary. The active spoofing attacker knows the authentication scheme and will try his best to imitate the walking pattern of the genuine user to spoof the healthcare system.

The main goal of our system is to detect spoofing attacks. In fact, there are many other possible attacks to such healthcare system. We discuss these possible attacks and corresponding solutions.

- Replay attack. an adversary first records a measurement trace from another person. Then he replays the data trace to the monitoring device to fool the healthcare monitoring system. This attack can be easily detected as discussed in [22].
- MITM attack. Although a MITM attack during communication between the device and server can be easily prevented, there is another type of MITM in which an adversary may build a MITM monitor which bridges the user's skin and a wearable device. For example, once it detects a response message indicating healthy problems such as high blood pressure, it will manipulate the data and transmit the forged data to the server. This type of attack can be addressed by the scheme in [22].
- Video analysis. Further potential threats include deriving the walking patterns by studying a video of the target's gait through computer vision techniques. We believe this is a potential vulnerability of unknown severity and leave it as future work.

## 3 System Architecture of KEH-Gait

### 3.1 System Overview

In this section, we first show the output voltage signal from KEH contains distinctive walking patterns of different users. Then we describe the proposed system in details.

Fig. 2 compares the output voltage signal from accelerometer, PEH and EEH generated by two subjects when they are walking. These figures provide a clear visual confirmation that the voltage signal from the energy harvester contains personalized patterns generated by the subjects. This observation is promising as our goal is to recognize different subjects based on the output voltage signal of the KEH when they are walking.

Now we are ready to describe the proposed system in details. As shown in Fig. 3, the whole procedure of KEH-Gait consists of three parts: signal pre-processing, offline dictionary training, and classification.

When the user is walking, we collect voltage signal from KEH and apply a SVD-based noise removal method to reduce noise. Then gait cycles are segmented from time series voltage signal and interpolated into the same length. The same optimized projection matrix (as used for training) is used to reduce the dimension of the test signal and provide the measurement vector $\tilde{y}_i = R_{opt}\, y_i$, $i = 1, 2, \ldots, k$, and $k$ is the number of obtained gait cycles.

During the offline dictionary training phase, we again apply noise reduction, gait cycle segmentation and interpolation to obtain the gait cycles from the test signal. All detected cycles are passed to unusual cycles deletion to remove outliers of gait cycles. The obtained gait cycles are used to form the training dictionary $A_0$ by dictionary learning technique. After dictionary learning, we further apply a column reduction approach [26] to obtain a optimized dictionary $A$ and a projection optimization algorithm [27] to

1. IDOMOVE: https://www.idomove.com/

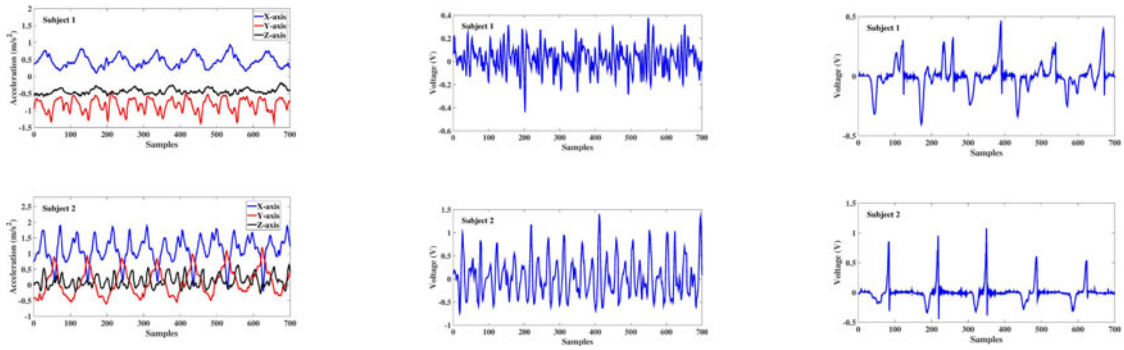


(a) Accelerometer signal (b) PEH voltage signal (c) EEH volage signal

Fig. 2. A comparison of the output signal from accelerometer, PEH and EEH: first row is the signal from subject 1 and the second row is the signal from subject 2.

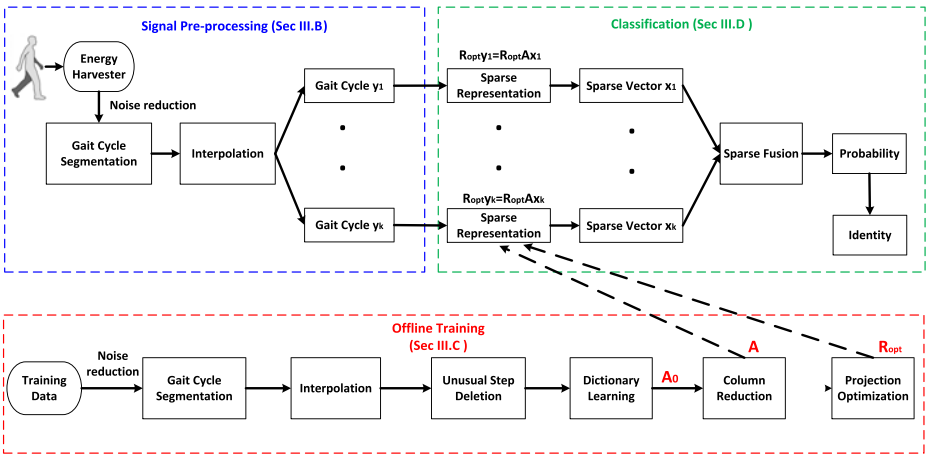


Fig. 3. System flowchart of KEH-Gait.

obtain a optimized projection matrix $R_{opt}$. Then the reduced training dictionary $\tilde{A} = R_{opt}\, A$ is used in the classifier as described in Section 3.4.

Now both the training dictionary $\tilde{A}$ and the measurements $\tilde{y}_i$ are passed to the classifier. The $\ell_1$ classifier first finds the sparse coefficient vector $x_i$. Then the vectors of different gait cycles are fused based on a novel probability-based sparse fusion model to calculate the probability of which class the test signal belongs to. Finally, the identity is obtained by finding the maximum probability $P$. The authentication can be achieved by comparing $P$ with a predefined threshold.

In the following sections, we provide more detailed descriptions of signal pre-processing, offline dictionary training, and classification in turn.

## 3.2 Signal Pre-Processing

### 3.2.1 SVD-Based Noise Reduction

In practical measurement, the collected voltage signal contains much noise. In the proposed system, we present a method to remove noise based on the decomposition of the data space into orthogonal subspaces through singular value decomposition (SVD). Because of the energy-preserving orthogonal transformation in the SVD, these subspaces correspond to the signal and noise components contained in the data. The noise reduction is obtained by suppressing the noise-related subspace and retaining the clean-signal space only.

Assume the voltage signal is $S = [s_1, s_2, \ldots, s_L]$, to achieve noise reduction, the Hankel-form matrix of the original noisy signal is defined as [28]:

$$H_{noisy} = \begin{bmatrix} s_1 & s_2 & \cdots & s_J \\ s_2 & s_3 & \cdots & s_{J+1} \\ \vdots & \vdots & \vdots & \vdots \\ s_I & s_{I+2} & \cdots & s_{I+J-1} \end{bmatrix}_{I \times J}. \quad (1)$$

The dimension of $H_{noisy}$ is $I \times J$, where $I + J = L + 1$ and $I \geq J$. The original Hankel-form matrix can be decomposed into two subspaces, i.e., the noise related subspace and clean signal subspace. By assuming an additive noise component in the noisy signal, we can obtain:

$$H_{noisy} = H_{signal} + H_{noise}, \quad (2)$$

where $H_{signal}$ is the original Hankel matrix without noise, and $H_{noise}$ is the additive noise component.

The method starts with a singular value decomposition of the matrix $H_{noisy}$:

$$H_{noisy} = U \sum V^T = \sum_{i=1}^{r} \delta_i u_i v_i^T, \quad (3)$$

where $U = [u_1, u_2, \ldots, u_I]$ and $V = [v_1, v_2, \ldots, v_J]$ are orthogonal matrices, i.e.,

$$UU^T = I_I \quad and \quad VV^T = I_{J,} \quad (4)$$

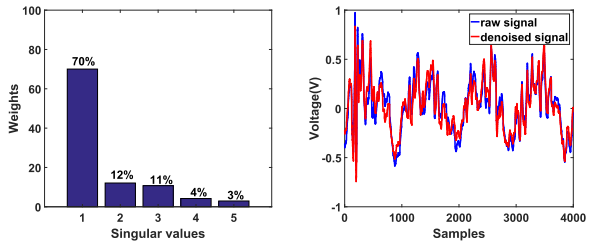


(a) (b)

Fig. 4. (a) Weights of singular values. (b) After noise reduction.

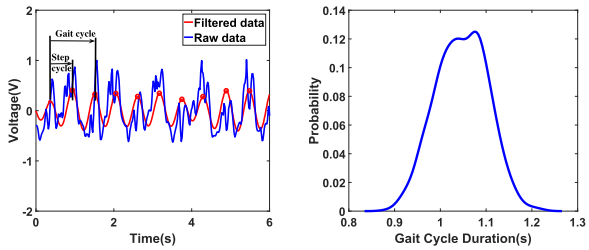


(a) (b)

Fig. 5. (a) Step detection. (b) Distribution of cycle duration.

$\sum$ is a diagonal matrix of singular values which has the following form:

$$\sum = \begin{bmatrix} \delta_1 & 0 & \cdots & 0 \\ 0 & \delta_2 & \cdots & 0 \\ \vdots & \vdots & \vdots & \vdots \\ 0 & 0 & \cdots & \delta_r \\ 0 & 0 & \cdots & 0 \\ \vdots & \vdots & \vdots & \vdots \\ 0 & 0 & \cdots & 0 \end{bmatrix}_{I \times J}. \quad (5)$$

The singular values $\delta_i$, i.e., the nonzero diagonal elements of $\sum$, are arranged in a descending order.

$$\delta_1 \geq \delta_2 \cdots \geq \delta_r \geq 0. \quad (6)$$

Theoretically, the largest singular value contributes almost only clean signal information, whereas the smallest singular value contributes almost only noise information. To obtain the clean signal, we should keep the largest $P$ singular values and discard the remaining singular values which are viewed as the noise components. To explain this, we plot the singular values of a series of voltage signal in Fig. 4a. We can see that the first 3 components contributes to 93 percent of the original signal, and the rest components are viewed as noise and should be discarded. Therefore, we adjust the singular values as follows:

$$\bar{\sum} = \begin{bmatrix} \delta_1 & 0 & \cdots & 0 & 0 & \cdots \\ 0 & \delta_2 & \cdots & 0 & 0 & \cdots \\ \vdots & \vdots & \vdots & \vdots & \vdots & \vdots \\ 0 & 0 & \cdots & \delta_P & 0 & \cdots \\ 0 & 0 & \cdots & 0 & 0 & \cdots \\ \vdots & \vdots & \vdots & \vdots & \vdots & \vdots \\ 0 & 0 & \cdots & 0 & 0 & 0 \end{bmatrix}_{I \times J}. \quad (7)$$

After this step, the signal after noise reduction can be obtained by:

$$H_{signal} = U\bar{\sum}V^T. \quad (8)$$

Fig. 4b shows the raw voltage signal and the denoised signal.

#### 3.2.2 Gait Cycle Segmentation

In order to recognize a gait signal, it is essential that we separate the time series of walking periods into segments, such that each segment contains a complete gait cycle. The gait cycle can be obtained by combining two successive step cycles together as technically the gait cycle is across a *stride* (two steps). As mentioned in [29], typical step frequencies are around 1-2 Hz, we apply a band-pass Butterworth filter [30] on the sampled data to eliminate out-band interference. The lower and upper cutoff frequency is set as 1 Hz and 2 Hz separately (filter order is 4). After filtering, the step cycles are separated by finding peaks associated with the heel strike as shown in Fig. 5a. Thereafter, the gait cycle is obtained by combining two consecutive step cycles together.

After gait cycle extraction, the output voltage data are segmented into short gait cycles based on the peak detection. Fig. 5b presents the distribution of cycle duration (i.e., time length of stride) for 20 healthy subjects walking at their normal speed. We can see that most of the gait cycle ranges between 0.8-1.3s (80-130 samples at 100 Hz sampling rate). This results in turn can be used to omit unusual gait cycles and exclude the cycles not produced by walking, i.e., the cycles which last less than 0.8s and exceed 1.3s are dropped.

#### 3.2.3 Linear Interpolation

Detected cycles are normalized to equal length by linear interpolation because the classifier requires vectors of equal length as input vector. As mentioned above, normal gait duration lies between 80 and 130 samples, we apply linear interpolation on the samples to ensure that they achieve the same length of 130 samples.

### 3.3 Offline Training

The training data are also passed to gait cycle segmentation and linear interpolation to obtain gait cycles with same length. In addition, we delete unusual cycles and optimize projection matrix to further improve recognition accuracy.

#### 3.3.1 Deletion of Unusual Cycles

Unusual cycles caused by occasional abnormalities like temporary walking pauses or turning contains much noise that will deteriorate the recognition accuracy. Apart from deleting unusual cycles using cycle durations, the detected cycles are also passed to a function which further deletes unusual cycles [31]. This function uses Dynamic Time Warping (DTW) distance scores to remove outliers from a set of cycles. Specifically, we first compute the DTW distance between the detected cycle and typical cycle. Thereafter, we delete unusual cycles by a simple threshold method, i.e., if the DTW distance of detected cycle and typical cycle is higher than a predefined value (12 in the proposed system), the detected cycle will be dropped. The typical cycle is the one which is assumed to represent the subject's gait signal. This is obtained by computing the the average of all cycles in the training data.

#### 3.3.2 Dictionary Construction

After unusual cycles removal, the remaining gait cycles obtained from training data are used to construct the training dictionary. Recent research shows that learning a dictionary by fitting a set of overcomplete basis vectors to a

collection of training samples can generate more compact and informative representation from given data and achieve better recognition accuracy [32]. We construct the training dictionary by dictionary learning technique. In particular, we first learn one single dictionary for each subject, which is formed by a set of basis vectors learned by solving a sparse optimization problem. Then we construct the full dictionary by concatenating single dictionaries together.

Note that because training examples and test samples are vectors, we will also refer to them as training vectors and test vectors. Suppose we have $K$ classes indexed by $i = 1, \ldots, K$ and each class $i$ contains $N$ training examples which are denoted as $S_i = \{s_1, s_2, s_3, \ldots, s_N\}$. Each training example is assumed to be a column vector with $q$ elements (i.e., feature dimension). For class $k$, we aim to find an over-complete dictionary matrix $A_k \in \mathbb{R}^{q \times N}$ over which a test vector has a sparse representation $X_k = \{x_1, x_2, \ldots, x_{N_i}\}$. After that, the raw training examples $S_i$ can be linearly expressed by $n_k$ vectors in $A_k$ where $n_k \ll N$. The optimization problem of training a dictionary can be formulated as:

$$\arg\min_{A_k, X_k} \|S_k - A_k X_k\|_2^2 \quad \text{subject to } \|x_i\|_0 \leq n_k. \tag{9}$$

There are several dictionary learning algorithms that can be used to train a dictionary such as MOD [33], K-SVD [32] and NMF [34]. In this study, we choose K-SVD because it is efficient, flexible and works in conjunction with any pursuit algorithms. The dictionary learning algorithm is detailed in Algorithm 1. After constructing a dictionary for each subject, we concatenate single dictionaries together to form the initial training dictionary $A_0 = [A_1, A_2, \ldots, A_K]$.

**Algorithm 1.** Subject-Specific Dictionary Learning

1: Input: Training samples $S = \{s_1, s_2, s_3, \ldots, s_N\}$, initial dictionary $A^0 \in \mathbb{R}^{q \times N}$, target sparsity $\tau$.
2: Output: Dictionary $A$ and sparse coefficients matrix $X$.
3: Initialization: set dictionary $A = A^0$.
4: **while** != stopping criteria **do**
5: $x_i = \arg\min_x \|s_i - x\|_2^2 \quad \text{s.t. } \forall i \quad \|Ax\|_0 \leq \tau$
6: **for** $j = 1, \ldots, N$ **do**
7: $J = \{$ *indices of the columns of* $X$ *orthogonal to* $w_j$ ($j$th *column of* $D$)$\}$
8: $w_j = \arg\min_w \|w^T A_J\|_2^2 \quad \text{s.t. } \|w\|_2 = 1$
9: $A(j\text{th } row) = w_j^T$;
10: **end for**
11: **end while**

### 3.3.3 Column Reduction and Projection Optimization

According to the formation of $\ell_1-$Homotopy, the computational complexity is $O(\tau^3 + \tau q(N \cdot K))$, where $\tau$ is the sparsity of the solution ($\tau \ll N \cdot K$), $q$ is the number of equations, and $N \cdot K$ is the number of unknowns, i.e., the number of columns in the training dictionary. We can see that the computation of $\ell_1$ optimization is also proportional to the number of columns $(N \cdot K)$ in the dictionary $A_0$. The gait cycles in the same class are highly correlated and lead to intra class redundancy. To reduce the intra class redundancy in the dictionary while retaining the most informative columns, we apply the columns reduction approach [26] to improve the efficiency and obtain an optimised dictionary $A$. Furthermore, motivated by a recent work [27], we apply the projection matrix optimization method proposed in [27] to reduce the dimensionality of SRC while retaining the high classification accuracy.

## 3.4 PMSSRC

SRC proposed in [35] aims to solve the classification problem of one test vector, however, the evaluation results in Section 5.3 show that the recognition accuracy of using one gait cycle can achieve 86 percent (PEH dataset) and 75 percent (EEH dataset) only. To overcome this limitation, we propose a novel probabilistic fusion model which fuses the information from multiple consecutive gait cycles to further improve recognition accuracy.

Suppose we have acquired a set of $M$ gait cycles $Y = \{y_1, y_2, \ldots, y_M\}$ from the test signal. Following the single test vector approach described in [35], we can obtain a set of estimated coefficients vectors $\hat{X} = \{\hat{x}_1, \hat{x}_2, \ldots, \hat{x}_M\}$ by solving the $\ell_1$ optimization problem for each gait cycle. Then we calculate the residual for each gait cycle as [35] and obtain $\Re = \{r_1, r_2, \ldots, r_M\}$. The probability of the $m$th test gait cycle belonging to the $i$th class is defined $p(\phi = i|y_m)$ where $\phi$ is used to denote the identity of $y_m$. Taking the elements of $Y$ as independent observations, the probability of all $M$ gait cycles belonging to $i$th class can be denoted by $p(\phi = i|Y)$.

As discussed in [35], the magnitude of $r_i$ represents the similarity between the test sample and $i$th subject. With this knowledge, we use the $\ell_1$-norm of the residual $r_i$ to define the posterior probability of $m = i$ given $y_m$ as follows:

$$p(\phi = i|y_m) = \frac{exp(-\lambda \|r_i\|_1)}{\sum_{j=1}^{M} exp(-\lambda \|r_j\|_1)} \in [0, 1], \tag{10}$$

where $\lambda$ is a constant parameter (0.3 in the proposed system).

For the $i$th subject, we define $\theta_i$ as

$$\theta_i = \sum_{y \in Y} lnp(\phi = i|y). \tag{11}$$

Since we have no prior knowledge of $y$, it should normally follow a uniform distribution over $1, 2, \ldots, M$, say $p(\phi = i) = 1/M$. We can obtain the probability of all $M$ gait cycles belonging to $i$th class $p(\phi = i|Y)$ as follows:

$$p(\phi = i|Y) = \frac{exp(\phi_i)}{\sum_{j=1}^{M} exp(\phi_j)} \in [0, 1]. \tag{12}$$

With the knowledge of $p(\phi = i|Y)$, the final classification result is obtained by finding the maximum posterior probability:

$$Identity = \max_i p(\phi = i|Y). \tag{13}$$

To identify whether the walker is the genuine user or imposter, we can make decision based on a threshold as:

$$p \begin{cases} \geq P_{th} & \text{genuine user} \\ < P_{th} & \text{imposter.} \end{cases}$$

where $P_{th}$ is a threshold we set empirically. An appropriate threshold can be chosen by data-driven approach to make the recognition system robust to imposters.

# 4 Hardware Platform and Data Collection

## 4.1 Proof-of-Concept Prototype

To this end, we built two data loggers to collect KEH voltage signals. One is based on piezoelectric energy harvester

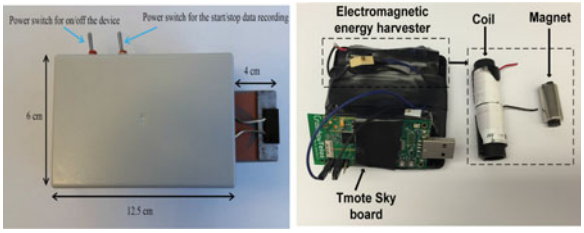


(a) (b)

Fig. 6. (a) PEH data logger and (b) EEH data logger.

(PEH) and the other is based on electromagnetic energy harvester (EEH). We encourage the reader to refer to [20] for background of PEH and EEH. The PEH data logger includes a vibration energy harvesting product from the MIDE Technology, which implements the transducer to provide AC voltage as its output. An Arduino Uno has been used as a microcontroller device for sampling the data from the Volture. The EEH data logger contains a harvesting circuit, through which energy is generated by moving a magnet through an inductor. A Tmote Sky board has been used as a microcontroller device for sampling the data from the inductor. In each prototype, we design a small amplification circuit to increase the range of output voltage (the original voltage range is 0.06-0.12V). Our hardware also includes a 3-axis accelerometer to record the acceleration signals, simultaneously with the voltage signal. For both KEH and accelerometer, a sampling rate of 100Hz has been used for data collection. The hardware platforms are shown in Fig. 6.

### 4.2 Data Collection

The dataset used to evaluate the performance of the proposed system consists of 20 healthy subjects (14 males and 6 females).[2] During the data collection phase, the participants were asked to hold the data logger in their preferred hand and walk at their normal speed (0.7-1.1m/s). The data collection is performed in several environments (indoor and outdoor) in order to capture the influence of different terrains. An illustration of indoor environment and outdoor environment is shown in Figs. 7a and 7b. The terrain of the chosen outdoor environment varies including plain, grass and asphalt. Each volunteer participated in two data collection sessions that was separated by one week. During each session, the participants were asked to hold the device (see Figs. 7c and 7d) and walked along the specific route shown in Figs. 7a and 7b for approximately 5 minutes. Based on the above description, the gait dataset is close to a realistic environment as it includes the natural gait changes over time and different environments (indoor and outdoor). In total, we collect over 600 seconds of samples for each subject from the EH devices as well as the accelerometer. We collect two voltage datasets by using the PEH and EEH devices, respectively, and perform gait cycle segmentation and unusual gait cycle deletion on both of the datasets, and finally we extract 200 gait cycles from each subject for evaluation.

## 5 Evaluation

### 5.1 Goals, Metrics and Methodology

In this section, we evaluate the performance of the proposed system based on the collected dataset. The goals of the evaluation are threefold: 1) investigate the relation between recognition accuracy and sampling rate of accelerometer data; 2) compare the recognition accuracy of KEH-Gait with that of using accelerometer data; 3) compare the proposed classification method in KEH-Gait with several state-of-the-art classification algorithms.

2. Ethical approval for carrying out this experiment has been granted by the corresponding organization (Approval Number HC15304 and HC15888).

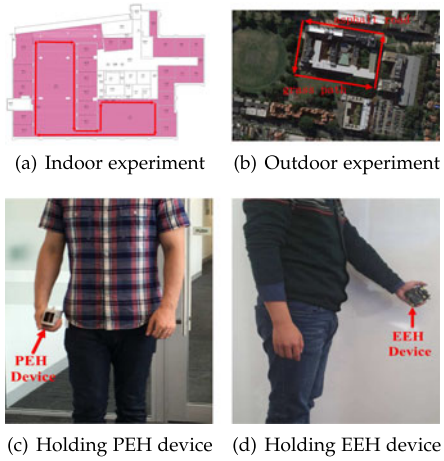


(a) Indoor experiment (b) Outdoor experiment

(c) Holding PEH device (d) Holding EEH device

Fig. 7. The illustration of data collection.

The recognition accuracy of KEH-Gait is obtained by using output voltage in one gait cycle as a test vector. For fair comparison, we perform the same signal processing and classification method on acceleration data. The only difference is the test vector is obtained by concatenating acceleration data along three axes in one gait cycle together. In the evaluation, we compare MSSRC with Support Vector Machine (SVM), K-Nearest Neighbor (KNN), and Naive Bayes (NB). The parameters in SVM, KNN and NB are well tuned to give highest accuracy. Specifically, we first separate the whole dataset into two parts: the training set which is used for parameter tuning, and validation set which is used for performance evaluation. We apply grid search to optimize hyperparameters via running internal 10-fold cross-validation on training set. For example, the range of penalty parameter $C$ for Linear kernel SVM classifier is $\{1, 10, 100, 1000\}$. Then we perform 10-fold cross-validation on the validation set to obtain the evaluation results using optimized parameters. For KNN classifier the number of nearest neighbors is 10. For SVM classifier, the best performance is obtained using linear kernel function ($C = 10$). The best performance of NB classifier is obtained using normal Gaussian distribution. In the evaluation, we let $k$ denote the number of gait cycles fused to perform classification and $\rho$ denote the compression rate. The compression rate means the number of projections/features over the dimension of original testing vector. We plot the results of the average values and 95 percent confidence level of the recognition accuracy obtained from 10 folds cross-validation.

### 5.2 Recognition Accuracy versus Sampling Rate

In the first experiment, we evaluate the impact of sampling rate on the gait recognition accuracy of acceleration data. The goal is to investigate the relation between recognition accuracy and the consumed power of accelerometer, as the power consumption is directly related to the sampling rate. We use PMSSRC as the classifier and calculate the recognition accuracy at different sampling rates by subsampling the acceleration data from 100 Hz to 1 Hz. As shown in Fig. 3, the recognition accuracy increases with growing sampling rate.

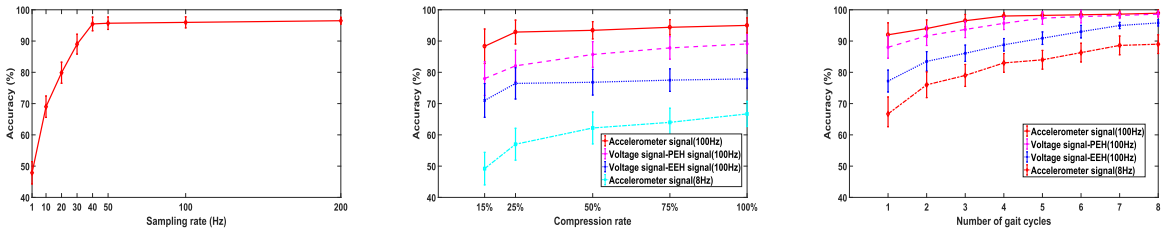


(a) (b) (c)

Fig. 8. (a) Recognition accuracy vs. sampling rate. (b) Recognition accuracy under different compression rate when k=1. (c) Recognition accuracy under different number of gait cycles when $\rho = 75$ percent.

This is intuitive as the more measurements are sampled, the more information is available, and thus, enabling more accurate classification. However, the improvement diminishes after the sampling rate is greater than 40 Hz. The results indicate that to achieve high recognition accuracy, a sampling rate of at least 40 Hz is required. In the rest of the evaluation, we limit our discussion on sampling at 40 Hz.

As we will discuss in Section 6.2.1, the power consumption of accelerometer-based system will increase significantly with the rising sampling frequency. Based on our measurement results, the accelerometer-based system consumes approximately 300 $\mu W$ with 40 Hz to achieve accurate recognition. However, this consumption requirement is far beyond the actual power generated by the energy harvester (neither PEH, nor EEH). According to a recent theoretical study of energy harvesting from human activity [12], assuming 100 percent conversion efficiency, the power can be harvested from walking is only 155 $\mu W$. Unfortunately, in practical, according to our measurement results, the average power produced from walking is 19.17 $\mu W$ using EEH, and approximately 1 $\mu W$ using PEH which is not tuned specifically for human activity energy harvesting. In this case, due to the limited amount of power that is available to power the system, its sampling frequency will decrease below 40Hz. According to our measurements, the accelerometer can at most sample at 25Hz with 155 $\mu W$ and 2 Hz with 19.17 $\mu W$. As a result, the recognition accuracy will dramatically decrease accordingly. The results highlight the necessity of using kinetic voltage signal to achieve gait recognition directly, instead of using the accelerometer signal.

### 5.3 KEH-Gait versus Accelerometer-Based System

In this section, we investigate whether KEH-Gait can achieve comparable accuracy compared to accelerometer signal. In case of using accelerometer signal, we calculate the recognition accuracy at two different sampling rates: 1) raw sampling rate (100 Hz) of the data logger; and 2) the highest achievable sampling rate of the accelerometer if it is powered by the energy harvester. From our dataset, the EEH can generate 19.17 $\mu W$ on average from walking. Thus, according to the handbook of MPU9250 which is used in our prototypes, it can sample at most 8 Hz if it is powered by the energy harvester.

In this experiment, we set $k = 1$ and calculate the recognition accuracy by varying compression rate $\rho$ from 15 to 100 percent, and the results are plotted in Fig. 8b. We can see that the recognition accuracy of using voltage signal is significantly higher than that of using accelerometer at sampling rate of 8 Hz. This suggests that the harvested power cannot support the accelerometer to sample at a high frequency which leads to low recognition accuracy; instead, using the voltage signal itself is able to achieve higher recognition accuracy. However, the recognition accuracy of using voltage signal is still approximately 6 percent (PEH) and 17 percent (EEH) below than that of using raw accelerometer signal when $\rho = 100$ percent.

We now demonstrate that the recognition accuracy of using harvested power signal can be improved significantly by the proposed PMSSRC, and it reaches a comparable recognition accuracy compared to using the raw accelerometer signal. In this experiment, we set $\rho = 75$ percent as the accuracy improvement diminishes when the number of projections/features increased to 200 as shown in Fig. 8b. Then we calculate the recognition accuracy of KEH-Gait using accelerometer signal and voltage signal, while increasing $k$ from 1 to 8. From the results in Fig. 8c, we notice that the recognition accuracy is improved significantly when more gait cycles are fused together. The result is intuitive as more information can be obtained to identify the subject by using more gait cycles. We also find that by using voltage signal of PEH, we can achieve a comparable accuracy compared to using raw accelerometer signal when $k \geq 5$, and the recognition accuracy of EEH is slightly lower (2 percent) than using raw accelerometer signal. In the real application, $k$ can be tuned by the healthcare company to satisfy their own needs. For example, a larger $k$ makes the system more secure to the imposters while it sacrifices user experience because it will take more time to collect required steps.

### 5.4 Comparison with Other Classification Methods

We now evaluate whether PMSSRC outperforms other state-of-the-art classification algorithms. Specifically, we compare MSSRC with SVM, KNN, and NB. We perform comparison on two datasets separately.

*Performance on PEH Dataset*. We follow the same experimental procedure in Section 5.3 to evaluate the recognition accuracy of different methods under different $d$ (number of projections/features). From Fig. 9a, we find that KEH-Gait improves recognition accuracy by up to 11.7 percent compared to the second best classification method (i.e., NB). We further evaluate the recognition accuracy of SVM, KNN and NB by combining several gait cycles together. As KEH-Gait utilizes multiple gait cycles to find the final classification result, we apply the majority voting scheme to achieve a fair comparison. Specifically, we first obtain the identity of each gait cycle by using SVM, KNN and NB, then we apply majority voting scheme to combine the results together, the subject with the highest voting is declared to be the recognized person. Again, we set $\rho = 75$ percent and calculate the recognition accuracy of different methods by varying $k$ from 1 to 5 (number of gait cycles). From the results in Fig. 9b, we find that KEH-Gait consistently achieves the best performance and is up to 15 percent more accurate than the second best approach (i.e., NB). The improvement of PMSSRC over other methods is because it exploits the sparsity information from multiple gait cycles.

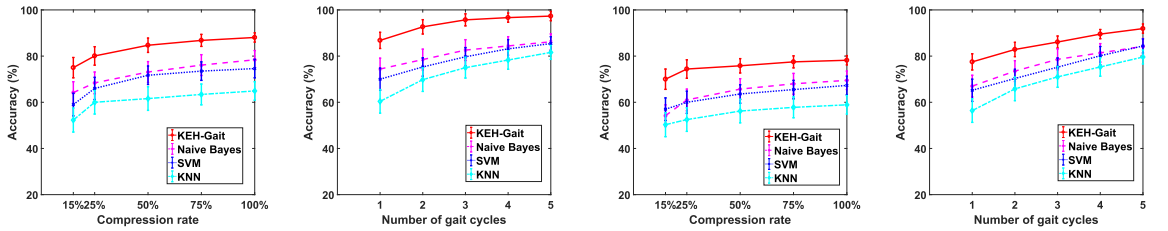


(a) PEH dataset with different compression rate ($k = 1$) (b) PEH dataset with different $k$ ($\rho = 0.75$) (c) EEH dataset with different compression rate ($k = 1$) (d) EEH dataset with different $k$ ($\rho = 0.75$)

Fig. 9. Comparison with other classification methods on two datasets (sample rate 40Hz).

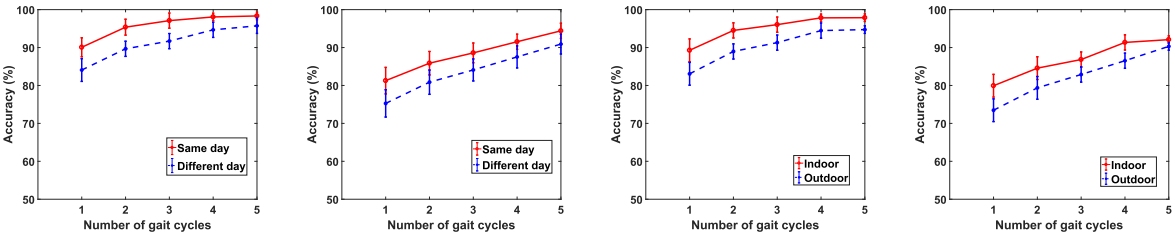


(a) PEH dataset (b) EEH dataset (c) PEH dataset (d) EEH dataset

Fig. 10. Robustness to gait variations.

*Performance on EEH Dataset.* We perform the same steps as above on EEH dataset and plot the results in Figs. 9c and 9d. The results show that KEH-Gait is 15.8 percent better than NB when $\rho = 75$ percent, $k = 1$, and 7.7 percent better than NB when $\rho = 75$ percent, $k = 5$. We also find that the overall performance on EEH dataset is lower than that on PEH dataset. We believe the drop on recognition accuracy is caused by the fact that the magnet is not sensitive to slight vibrations and motions.

The results in this section suggest that the proposed PMSSRC in KEH-Gait can improve recognition accuracy significantly by fusing several steps together and outperformS several state-of-the-art classification algorithms. Another straightforward method to apply SRC on multiple steps is to first apply SRC on each step and then obtain the final results by majority voting scheme. We found that PMSSRC is approximately 5–9 percent more accurate than direct majority voting on our dataset since it exploits the sparsity information of multiple measurements. Due to limited space, we do not plot the results of direct major voting in this paper.

### 5.5 Robustness to Gait Variations

To evaluate the robustness of KEH-Gait to gait variations, we conduct the following two experiments: different day evaluation and different environment evaluation. In this experiment, same day evaluation means the training set and test set are chosen from the sessions of the same day while different days evaluation chooses the sessions from two different days separated by 1 week. Similarly, in different environment evaluations, indoor evaluation means the training set and test set are chosen from indoor environment while outdoor evaluation chooses training data and test data from outdoor environment. We conduct this evaluation on PEH dataset and EEH dataset respectively. As the results in Figs. 10a and 10b, the accuracy of different day is lower than the same day evaluation as the different days evaluation tends to produce more changes to gait. However, KEH-Gait can still achieve the accuracy of 96 and 91 percent on the two dataset respectively when more than 4 steps are used. This observation holds in the different environment evaluation. From Figs. 10c and 10d, we can see outdoor environment achieves lower accuracy than indoor environment because it includes several different terrains such as grass path and asphalt road. Gait changes can be caused many other factors such as speed and shoes etc. We have discussed the influence of these factors in [20].

### 5.6 Robustness against Attackers

As mentioned in Section 2, we assume the presence of a passive adversary and an active attacker during an authentication session. We evaluate the robustness of the proposed system against the eavesdropper and active attacker by conducting the following two imposter attempt experiments.

- A passive imposter attempt is an attempt when an imposter performs authentication using his own walking pattern. This attack happens when the genuine user passes his device to another person to spoof the healthcare system.
- An active imposter attempt means the imposter mimics the gait of the genuine user with the aim to spoof the healthcare system. This attack happens when the several users collude to fool the healthcare system.

In the passive imposter experiment, we separate the 20 participants into two groups: 10 of them are candidate users and the rest 10 subjects are attackers. We use the raw voltage signal from other subjects as passive imposter attempts. Therefore, there are $10 * 100 = 1000$ training samples and $10 * 100(positive) + 10 * 200(negative) = 3000$ test samples. To evaluate the robustness against the second imposter attack scenario, we group the 20 subjects into 10 pairs. Each subject was told to mimic his/her partner's walking style and try to imitate him or her. First, one participant of the pair acted as an imposter, the other one as a genuine user, and then the roles were exchanged. The genders of the imposter and the user were the same. They observed the walking style of the target visually, which can be easily done in a real-life situation as gait cannot be hidden. Every attacker made 5 active imposter attempts and each imposter attempt contains 20 gait cycles. Therefore, there are $10 * 100 = 1000$ training samples and $10 * 100(positive) + 10 * 5 * 20(negative) = 2000$ test samples. We set $k = 5$ and vary the confidence threshold $P$th to plot DET curve in Fig. 10.

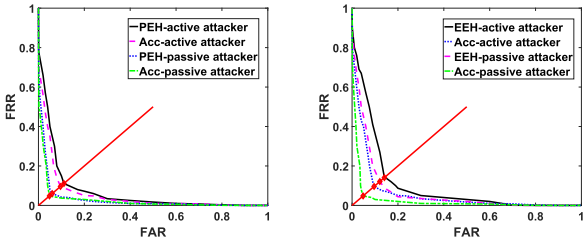


(a) PEH dataset (b) EEH dataset

Fig. 11. Robustness against attackers.

The results on two dataasets are plotted in Figs. 11a and 11b respectively. The crossover (marked as a diamond) of the red dash line and FPR-FNR curve stands for the location of the EER. We notice that EER of KEH-Gait is 6 and 12.1 percent on the two datasets respectively, which means out of 100 passive imposter trials 6 are wrongfully accepted by using PEH and 12 are wrongfully accepted by using EEH. We also find that an imposter does benefit from mimicking the genuine user's walking style. The EER increases to 11.2 and 14.1 percent on the two datasets respectively. For the accelerometer-based system, the EER of a passive attacker and an active attacker are 4.8 and 9.4 percent, respectively. The results indicate that the PEH-based system can achieve comparable EER compared to the accelerometer-based system. The individual nature of gait provides our scheme security against impersonation attackers and the evaluation results are encouraging. The false positives occur when the gait patterns of the imposter and user are close.

## 6 Energy Consumption Profile

In this section, we will conduct an extensive energy consumption profiling to analyze the energy consumption of our system and accelerometer-based system. The energy consumption of our system consists of three parts: sensor sampling, memory reading/writing, and data transmission. We find that memory reading/writing consumes significant less energy compared to the other two parts. A recent study [36] also investigates the energy consumption of different Random Access Memory (RAM) technologies, and their findings support our measurement results. According to their measurement, it only consumes 203pJ to write to (or read from) Static Random Access Memory (SRAM) which is used in SensorTag. That means if we collect 4s gait data at 40 Hz, it only takes $4 \times 40 \times 203 = 32.48$ nJ to read or write data. Compared to the energy consumption of other parts, the energy consumed by SRAM is negligible. Therefore, we only consider the energy consumption of sensor sampling and data transmission in our evaluation.

### 6.1 Measurement Setup

The Texas Instrument SensorTag is selected as the target device, which is embedded with the ultra-low power ARM Cortex-M3 MCU that is widely used by today's mainstream wearable devices such as FitBit. The SensorTag is running with the Contiki 3.0 operating system. The experiment setup for the power measurement is shown in Fig. 12a. In order to capture both the average current and the time requirement for each sampling event, the Agilent DSO3202A oscilloscope is used. As shown in the figure, we connect the SensorTag with a 10Ω resistor in series and power it using a 3V coin battery. The oscilloscope probe is then connected across the resistor to measure the current going through.

### 6.2 Energy Consumption of Sensor Sampling

#### 6.2.1 Power Consumption of Sampling Accelerometer

The SensorTag includes 9-axis digital MPU9250 motion sensor combining gyroscope, digital compass, and accelerometer. During the power measurements, we only enable the 3-axis accelerometer and leave all the other sensors turned off. The acceleration signal is sampled using the Inter-Integrated Circuit ($I^2C$) bus with a sampling frequency of 25 Hz. Note that, it is also possible for the wearable devices to use analog accelerometers, which can be sampled through analog-to-digital converter (ADC) instead of $I^2C$ bus. Sampling analog accelerometers could avoid power consumption and additional time requirement due to the $I^2C$ bus, but at the expense of some processing costs in analog to digital converting. While it is not immediately obvious whether analog accelerometer sampling would be less or more power consuming relative to the digital counterpart, a detailed measurement study [37] indicates that digital accelerometer is more power efficient than the comparable analog ones from the same manufacturers.

Fig. 12b shows the details of accelerometer sampling energy profile. As shown, each accelerometer sampling event can be divided into six states. At the beginning of each event, the MCU is waked up by the software interrupt from the power-saving deep-sleep mode (S_sleep), and it boots the accelerometer (S1) before going back to sleep. During S2, the accelerometer starts to power up while the MCU is in sleep mode. Then, after one software clock tick (7.8 ms in Contiki OS), the MCU wakes up again by the interrupt to initialize the accelerometer (S3) and then goes back to sleep. The accelerometer starts initializing in S4 and turning on in S5. Finally, MCU wakes up in S6 to sample the acceleration signal and then goes back to deep-sleep again. The average power consumption and time requirement for each state are shown in Table 1.

#### 6.2.2 Power Consumption of Sampling KEH

In this section, we investigate the power consumption in sampling the voltage signal of the power source. During the measurement, MCU is programmed to periodically sample

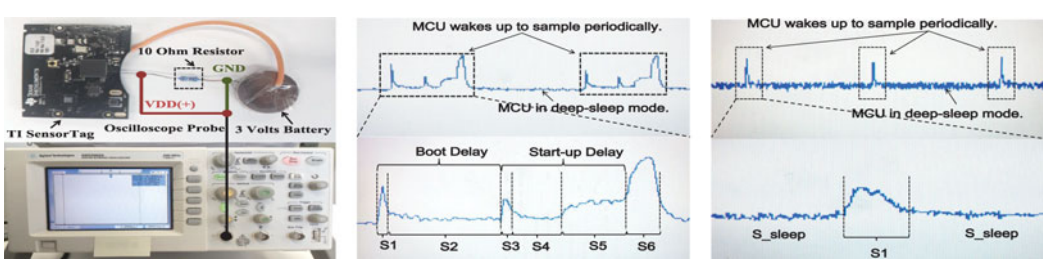


(a) Experimental setup. (b) Profiling of acceleration. (c) Profiling of voltage.

Fig. 12. Measurement setup and results.

TABLE 1
States of Accelerometer Sampling

| State | Time (ms) | Power (uW) |
|---|---|---|
| S1 | 0.6 | 768 |
| S2 | 7.2 | 72 |
| S3 | 0.6 | 480 |
| S4 | 3.2 | 72 |
| S5 | 4 | 480 |
| S6 | 1.6 | 1440 |
| S_sleep | null | 6 |

TABLE 2
States of Voltage Sampling

| State | Time (ms) | Power ($\mu$W) |
|---|---|---|
| S1 | 0.6 | 480 |
| S_sleep | null | 6 |

the voltage of the lithium coin battery with 25Hz sampling rate. The MCU reads voltage signal through ADC. Fig. 12 shows the details of voltage sampling. Similar to the accelerometer, the MCU goes back to deep-sleep mode after each sampling event. However, sampling the voltage takes only 0.6 ms, which is much shorter than the 17.2 ms required by the accelerometer sampling. This is because the MCU can read the voltage signal directly without having to prepare the hardware to be powered-up, and the voltage signal to be prepared by the power source. The details of power consumption and time duration for voltage sampling event are shown in Table 2.

#### 6.2.3 Energy Consumption Comparison

We now compare the energy consumption of sampling accelerometer and KEH. In general, for the duty-cycled gait-recognition system, the average power consumption in data sampling, $P_{sense}$, can be obtained by the following equation:

$$P_{sense} = \begin{cases} \frac{T_S \times n}{1000} P_{sample} + (1 - \frac{T_S \times n}{1000}) P_{sleep} & \text{if } 0 \leq n \leq \frac{1000}{T_S}, \\ P_{sample} & \text{if } \frac{1000}{T_S} < n. \end{cases} \quad (14)$$

where, $P_{sample}$ is the average power consumption in the sampling event (either sampling acceleration or KEH signal), and $P_{sleep}$ is the average power consumption when the MCU is in deep-sleep mode (with all the other system components power-off). $n$ is the sampling frequency, and $T_S$ is the duration of time (in milli-second) spent in a single sampling event. Based on the measurement results given in Tables 1 and 2, we can obtain the average power consumption for the accelerometer sampling event equals to 322 $\mu$W with a time requirement of 17.2 ms, and 480 $\mu$W with a duration of 0.6ms for the KEH sampling event. Then, based on Equation (14), we get the power consumption in data sampling for both accelerometer-based and KEH-based gait-recognition systems with different sampling frequencies. The results are compared in Fig. 13. It is clear to see that the proposed KEH-Gait achieves significant power saving in data sampling, comparing with the conventional accelerometer-based gait-recognition system. More specifically, given the analysis shown in Fig. 8a, a sampling rate higher than 40 Hz is needed to achieve high recognition accuracy. With a 40 Hz sampling frequency, in case of data

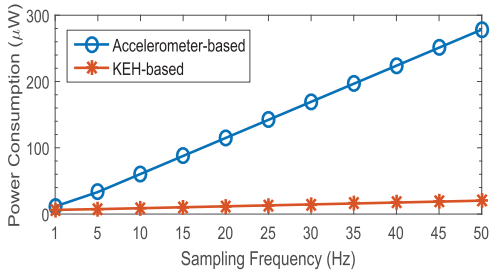


Fig. 13. Power consumption comparison.

sampling, KEH-Gait consumes 17.38 $\mu$W, while the power consumption of accelerometer-based system is 230.74 $\mu$W.

As can be seen from Fig. 8c, to achieve more than 95 percent accuracy, it needs to collect 3 gait cycles for the accelerometer-based system and 4 gait cycles for the KEH-based system. If we assume one gait cycle takes 1s (the average time of one gait cycle is between 0.8s-1.2s), this results in 69.52 $\mu$J and 692.22 $\mu$J energy consumption in data sampling for KEH-Gait and accelerometer-based system, respectively.

### 6.3 Energy Consumption of Data Transmission

Next, we evaluate the energy consumption of transmitting acceleration and KEH voltage data via Bluetooth. We conduct power measurement of the Bluetooth Low Energy (BLE) beacon using the embedded CC2650 wireless MCU in the SensorTag. With the 40 Hz sampling rate, KEH-Gait generates 160 voltage samples every four seconds. If we set compression rate to 75 percent, this results in 240 bytes data to be transmitted in total (2 bytes for each of the 12-bits ADC voltage reading). This consumes an average power of 1.99 mW with a transmission time of 44.28 ms, which results in 88.12 $\mu$J of energy consumption. On the other hand, as 3-axis acceleration data is collected for 3s, it results in 540 bytes of data and the energy consumption of transmitting those data is 190.94 $\mu$J.

After obtaining the energy consumption of sensor sampling and data transmission, we investigate the potential of KEH-Gait for energy saving. Based on the measured results, the energy consumption of KEH-Gait to complete one authentication is approximately 157.64 $\mu$J, which has reduced the energy consumption of the accelerometer-based system (883.16 $\mu$J) by 82.15 percent. In the proposed system, the time-consuming classification task will be executed in the server; therefore, we do not need to evaluate the processing time and latency of the system.

## 7 Discussion

Many factors exist that may impact the accuracy of a gait-based recognition system, such as shoe, clothes, walking speed and terrain. Previous studies have shown that the accuracy will decrease when the test and training samples of the person's walking are obtained using different shoe types and clothes [38]. Indeed, as shown in Section 5.5, the accuracy of KEH-Gait decreases when session 1 is used for training and session 2 is used for testing. The dataset used in the experiment is challenging as it includes the natural gait changes over time (two sessions separated by 1 week), as well as gait variations due to changing in clothes, terrain and shoes. However, KEH-Gait can still achieve the accuracy of 95 and 89 percent on the two dataset respectively by the proposed MSSRC, which in turn demonstrate the robustness of KEH-Gait to gait variations. The focus of our

study is to demonstrate the feasibility of gait recognition using KEH and improve its performance. Due to space limitation, we defer the analysis of different factors to our future work. In fact, there has been several attempts to study the relationship between recognition performance and different factors [31], [38]. For example, in terms of walking speed, Muaaz and Nickel [31] found that normal walk has best results and fast walk is a bit better than slow walk. As for different types of terrains, they reported that gravel walk has better results than grass and inclined walk. We encourage the reader to refer to [31], [38], [39] for more details. One major limitation of our work is that we only collect data from hand due to hardware limitation. As wearable devices can be worn in many other positions like waist, foot and pocket, our future work will focus on evaluating the performance of the system on different positions.

## 8 Related Work

*Gait Recognition*. Gait recognition has been well studied in the literature. From the way how gait is collected, gait recognition can be categorized into three groups: vision based, floor sensor based, and wearable sensor based. In vision based gait recognition system, gait is captured from a remote distance using video-camera. Then, video/image processing techniques are employed to extract gait features for further recognition. A large portion in the literature belong to this category [40], [41], [42], [43]. In floor sensor based gait recognition, sensors (e.g., force plates), which are usually installed under the floor, are used for capturing gait features, such as ground reaction force (GRF) [44] or heel-to-toe ratio [45].

Compared with vision-based and other non-accelerometer based gait measurements, acceleration can reflect the dynamics of gait more directly and faithfully. The first work of accelerometer based gait recognition is proposed by Ailisto et al. [9] and further developed by Gafurov et al. [46]. In the initial stages, dedicated accelerometers were used and worn on different body positions, such as lower leg [46], waist [9], hip [47], hip pocket, chest pocket and hand [48]. With the prevailing of smartphone, researchers have proposed several gait-based authentication systems by utilizing the built-in accelerometer [6], [49], [50]. In a previous work, the researchers analyzed human gait by a shoe-embedded piezoelectric energy harvester [51].

Recognition can be performed in two ways: (a) by pattern similarity matching based on gait template or (b) by machine-learning (ML) approaches where gait recognition is represented as classification problem. Approaches that are based on template matching usually rely on simple metrics that measure dissimilarity of compared gait patterns, including histogram similarity [46], euclidean distance [52] and DTW distance [53]. Approaches where gait recognition is carried out as a classification problem, rely on commonly used classification techniques, including k-NN [54], SVM [55], decision trees [56], random forests [57] and neural networks [58]. In this paper, we propose PMSSRC and the evaluation results show that it outperforms classic classifiers.

*Biometric Cryptosystems (BCS)*. Our work is also closely related to biometric cryptosystems (BCS) which are developed for the purpose of either securing a cryptographic key using biometric features or directly generating a cryptographic key from biometric features. Recently there are several studies using gait to generate secret keys. For example, Hoang et al. used gait to encrypt a cryptographic key through a fuzzy commitment scheme [25]. In a similar work [59], Xu et al. proposed an automatic key generation system for on-body devices by using gait. After that, Schürmann et al. proposed a device-to-device authentication system for body area network using natural gait [60]. Revadigar et al. proposed a group key generation protocol for on-body devices by fuzzy vault [61].

*Studies on KEH*: Recently researchers are investigating to use the output signal from KEH to achieve a wide range of applications in activity tracking [62], transportation mode detection [63], and acoustic communication [64]. In [62], the authors proposed the idea of using the energy harvesting power signal for human activities recognition. In [63], the authors proposed to use KEH to detect different transportation mode. Following this trend of study, the proposed KEH-Gait utilizes the voltage signal generated by the kinetic energy harvester from walking to perform gait recognition. We also discuss the limitations and advantages of using KEH for gait recognition in [20].

## 9 Conclusion

In this paper, we explore the feasibility of using KEH to address the problem of user spoofing attacks in emerging mobile healthcare systems. Compared to accelerometer-based system, KEH-Gait is able to achieve comparable recognition accuracy when multiple steps are used and reduce energy consumption by 82.15 percent. Moreover, the security analysis shows that the EER of KEH-Gait against an active spoofing attacker is 11.2 and 14.1 percent on the two datasets respectively. Our study results show that the output voltage signal of energy harvester is a promising informative signal for wearable authentication system. Although health monitoring was used as the main motivating scenario for this work, we believe the proposed KEH-based gait detection could be influential to many other scenarios. For example, KEH can be used in consumer electronics to enable many other applications due to the nature of energy savings.

## References

[1] F. Albinali, S. Intille, W. Haskell, and M. Rosenberger, "Using wearable activity type detection to improve physical activity energy expenditure estimation," in *Proc. 12th ACM Int. Conf. Ubiquitous Comput.*, 2010, pp. 311–320.

[2] J. Lester, C. Hartung, L. Pina, R. Libby, G. Borriello, and G. Duncan, "Validated caloric expenditure estimation using a single body-worn sensor," in *Proc. 11th Int. Conf. Ubiquitous Comput.*, 2009, pp. 225–234.

[3] J.-Q. Li, F. R. Yu, G. Deng, C. Luo, Z. Ming, and Q. Yan, "Industrial internet: A survey on the enabling technologies, applications, and challenges," *IEEE Commun. Surveys Tuts.*, vol. 19, no. 3, pp. 1504–1526, Jul.-Sep. 2017.

[4] M. Rabbi, S. Ali, T. Choudhury, and E. Berke, "Passive and in-situ assessment of mental and physical well-being using mobile sensors," in *Proc. ACM Int. Conf. Ubiquitous Comput.*, 2011, pp. 385–394.

[5] C. Luo, H. Hong, M. C. Chan, J. Li, X. Zhang, and Z. Ming, "Mpiloc: Self-calibrating multi-floor indoor localization exploiting participatory sensing," *IEEE Trans. Mobile Comput.*, vol. 17, no. 1, pp. 141–154, Jan. 2018.

[6] Y. Ren, Y. Chen, M. C. Chuah, and J. Yang, "Smartphone based user verification leveraging gait recognition for mobile healthcare systems," in *Proc. IEEE Int. Conf. Sensing Commun. Netw.*, 2013, pp. 149–157.

[7] Y. Ren, J. Yang, M. C. Chuah, and Y. Chen, "Mobile phone enabled social community extraction for controlling of disease propagation in healthcare," in *Proc. IEEE 8th Int. Conf. Mobile Ad-Hoc Sensor Syst.*, 2011, pp. 646–651.

[8] D. Gafurov, K. Helkala, and T. Søndrol, "Gait recognition using acceleration from mems," in *Proc. First 1st Int. Conf. Availability Rel. Security*, 2006, pp. 6–12.

[9] H. J. Ailisto, M. Lindholm, J. Mantyjarvi, E. Vildjiounaite, and S.-M. Makela, "Identifying people from gait pattern with accelerometers," in *Proc. Defense Security*, 2005, pp. 7–14.

[10] Y. Zhang, G. Pan, K. Jia, M. Lu, Y. Wang, and Z. Wu, "Accelerometer-based gait recognition by sparse representation of signature points with clusters," *IEEE Trans. Cybern.*, vol. 45, no. 9, pp. 1864–1875, Sep. 2015.

[11] M. Rostami, A. Juels, and F. Koushanfar, "Heart-to-heart (h2h): Authentication for implanted medical devices," in *Proc. ACM Conf. Comput. Commun. Security*, 2013, pp. 1099–1112.

[12] M. Gorlatova, J. Sarik, G. Grebla, M. Cong, I. Kymissis, and G. Zussman, "Movers and shakers: Kinetic energy harvesting for the internet of things," in *Proc. ACM SIGMETRICS Perform. Eval. Rev.*, vol. 42, no. 1, 2014, pp. 407–419.

[13] T. Von B üren, P. D. Mitcheson, T. C. Green, E. M. Yeatman, A. S. Holmes, and G. Tröster, "Optimization of inertial micropower generators for human walking motion," *IEEE Sensors J.*, vol. 6, no. 1, pp. 28–38, Feb. 2006.

[14] J. Yun, S. N. Patel, M. S. Reynolds, and G. D. Abowd, "Design and performance of an optimal inertial power harvester for human-powered devices," *IEEE Trans. Mobile Comput.*, vol. 10, no. 5, pp. 669–683, May 2011.

[15] P. D. Mitcheson, E. M. Yeatman, G. K. Rao, A. S. Holmes, and T. C. Green, "Energy harvesting from human and machine motion for wireless electronic devices," *Proc. IEEE*, vol. 96, no. 9, pp. 1457–1486, Sep. 2008.

[16] S. Khalifa, M. Hassan, and A. Seneviratne, "Pervasive self-powered human activity recognition without the accelerometer," in *Proc. IEEE Int. Conf. Pervasive Comput. Commun.*, 2015, pp. 79–86.

[17] A. Bilbao, D. Hoover, J. Rice, and J. Chapman, "Ultra-low power wireless sensing for long-term structural health monitoring," *Proc. Sens. Smart Struct. Technol. Civil Mech. Aerosp. Syst.*, 2011, pp. 798 109–79814.

[18] AMPY, [Online]. Available: http://www.getampy.com/ampy-move.html//, accessed on 30 Apr. 2017.

[19] SOLEPOWER, [Online]. Available: http://www.solepowertech.com/#new-page//, accessed on 30 April 2017.

[20] W. Xu, G. Lan, Q. Lin, S. Khalifa, N. Bergmann, M. Hassan, and W. Hu, "Keh-gait: Towards a mobile healthcare user authentication system by kinetic energy harvesting," in *Proc. Netw. Distrib. Syst. Security Symp.*, 2017, pp. 1–15.

[21] S. Ravi, A. Raghunathan, and S. Chakradhar, "Tamper resistance mechanisms for secure embedded systems," in *Proc. IEEE 17th Int. Conf. VLSI Des.*, 2004, pp. 605–611.

[22] L. Guan, J. Xu, S. Wang, X. Xing, L. Lin, H. Huang, P. Liu, and W. Lee, "From physical to cyber: Escalating protection for personalized auto insurance," in *Proc. 14th ACM Conf. Embedded Netwo. Sens. Syst. CD-ROM*, 2016, pp. 42–55 .

[23] H. Liu, S. Saroiu, A. Wolman, and H. Raj, "Software abstractions for trusted sensors," in *Proc. 10th Int. Conf. Mobile Syst. Appl. Services*, 2012, pp. 365–378.

[24] D. Donoho, "Compressed sensing," *IEEE Trans. Inf. Theory*, vol. 52, no. 4, pp. 1289–1306, Apr. 2006.

[25] T. Hoang, D. Choi, and T. Nguyen, "Gait authentication on mobile phone using biometric cryptosystem and fuzzy commitment scheme," *Int. J. Inf. Security*, vol. 14, no. 6, pp. 549–560, 2015.

[26] B. Wei, M. Yang, Y. Shen, R. Rana, C. T. Chou, and W. Hu, "Real-time classification via sparse representation in acoustic sensor networks," in *Proc. 11th ACM Conf. Embedded Netw. Sens. Syst.*, 2013, Art. no. 21.

[27] Y. Shen, W. Hu, M. Yang, B. Wei, S. Lucey, and C. T. Chou, "Face recognition on smartphones via optimised sparse representation classification," in *Proc. IEEE 13th Int. Symp. Inf. Process. Sensor Netw.*, 2014, pp. 237–248.

[28] K.-C. Lee, J.-S. Ou, and M.-C. Fang, "Application of svd noise-reduction technique to pca based radar target recognition," *Progress Electromagn. Res.*, vol. 81, pp. 447–459, 2008.

[29] A. Brajdic and R. Harle, "Walk detection and step counting on unconstrained smartphones," in *Proc. ACM Int. Joint Conf. Pervasive Ubiquitous Comput.*, 2013, pp. 225–234.

[30] S. Butterworth, "On the theory of filter amplifiers," *Wireless Engineer*, vol. 7, no. 6, pp. 536–541, 1930.

[31] M. Muaaz and C. Nickel, "Influence of different walking speeds and surfaces on accelerometer-based biometric gait recognition," in *Proc. IEEE. 35th Int. Conf. Telecommun. Signal Process.*, 2012, pp. 508–512.

[32] M. Aharon, M. Elad, and A. Bruckstein, "K-SVD: An algorithm for designing overcomplete dictionaries for sparse representation," *IEEE Trans. Signal Process.*, vol. 54, no. 11, pp. 4311–4322, Nov. 2006.

[33] K. Engan, S. O. Aase, and J. H. Husøy, "Multi-frame compression: Theory and design," *Signal Process.*, vol. 80, no. 10, pp. 2121–2140, 2000.

[34] D. D. Lee and H. S. Seung, "Algorithms for non-negative matrix factorization," in *Proc. Advances Neural Inf. Process. Syst.*, 2001, pp. 556–562.

[35] J. Wright, A. Yang, A. Ganesh, S. Sastry, and Y. Ma, "Robust face recognition via sparse representation," *IEEE Trans. Pattern Anal. Mach. Intell.*, vol. 31, no. 2, pp. 210–227, Feb. 2009.

[36] M. Moreau, "Estimating the energy consumption of emerging random access memory technologies," Master's thesis, Institutt for elektronikk og telekommunikasjon, 2013.

[37] F. Büsching, U. Kulau, M. Gietzelt, and L. Wolf, "Comparison and validation of capacitive accelerometers for health care applications," *Comput. Methods Programs Biomed.*, vol. 106, no. 2, pp. 79–88, 2012.

[38] S. Enokida, R. Shimomoto, T. Wada, and T. Ejima, "A predictive model for gait recognition," in *Proc. Biometrics Symp.: Special Session Res. Biometric Consortium Conf.*, 2006, pp. 1–6.

[39] D. Gafurov and E. Snekkenes, "Gait recognition using wearable motion recording sensors," *EURASIP J. Advances Signal Process.*, vol. 2009, 2009, Art. no. 7.

[40] T. H. Lam and R. S. Lee, "A new representation for human gait recognition: Motion silhouettes image (msi)," in *Proc. Int. Conf. Biometrics*, 2005, pp. 612–618.

[41] A. Kale, A. Sundaresan, A. Rajagopalan, N. P. Cuntoor, A. K. Roy-Chowdhury, V. Krüger, and R. Chellappa, "Identification of humans using gait," *IEEE Trans. Image Process.*, vol. 13, no. 9, pp. 1163–1173, Sep. 2004.

[42] Z. Liu and S. Sarkar, "Improved gait recognition by gait dynamics normalization," *IEEE Trans. Pattern Anal. Mach. Intell.*, vol. 28, no. 6, pp. 863–876, Jun. 2006.

[43] J. Han and B. Bhanu, "Individual recognition using gait energy image," *IEEE Trans. Pattern Anal. Mach. Intell.*, , vol. 28, no. 2, pp. 316–322, Feb. 2006.

[44] R. J. Orr and G. D. Abowd, "The smart floor: A mechanism for natural user identification and tracking," in *Proc. Extended Abstracts Human Factors Comput. Syst.*, 2000, pp. 275–276.

[45] L. Middleton, A. Buss, A. Bazin, M. S. Nixon, et al., "A floor sensor system for gait recognition," in *Proc. 4th IEEE Workshop Autom. Identification Advanced Technol.*, 2005, pp. 171–176.

[46] D. Gafurov, K. Helkala, and T. Søndrol, "Biometric gait authentication using accelerometer sensor," *J. Comput.*, vol. 1, no. 7, pp. 51–59, 2006.

[47] D. Gafurov, E. Snekkenes, and T. E. Buvarp, "Robustness of biometric gait authentication against impersonation attack," in *OTM 2006 Workshops On the Move to Meaningful Internet Systems.* Berlin, Germany: Springer, 2006, pp. 479–488.

[48] E. Vildjiounaite, S.-M. Mäkelä, M. Lindholm, R. Riihimäki, V. Kyllönen, J. Mäntyjärvi, and H. Ailisto, "Unobtrusive multimodal biometrics for ensuring privacy and information security with personal devices," in *Proc. Int. Conf. Pervasive Comput.*, 2006, pp. 187–201.

[49] H. Lu, J. Huang, T. Saha, and L. Nachman, "Unobtrusive gait verification for mobile phones," in *Proc. ACM Int. Symp. Wearable Comput.*, 2014, pp. 91–98.

[50] C. Luo, L. Cheng, M. C. Chan, Y. Gu, J. Li, and Z. Ming, "Pallas: Self-bootstrapping fine-grained passive indoor localization using wifi monitors," *IEEE Trans. Mobile Comput.*, vol. 16, no. 2, pp. 466–481, Feb. 2017.

[51] J. Zhao and Z. You, "A shoe-embedded piezoelectric energy harvester for wearable sensors," *Sens.*, vol. 14, no. 7, pp. 12 497–12 510, 2014.

[52] L. Rong, D. Zhiguo, Z. Jianzhong, and L. Ming, "Identification of individual walking patterns using gait acceleration," in *Proc. IEEE 1st Int. Conf. Bioinf. Biomed. Eng.*, 2007, pp. 543–546.

[53] N. T. Trung, Y. Makihara, H. Nagahara, R. Sagawa, Y. Mukaigawa, and Y. Yagi, "Phase registration in a gallery improving gait authentication," in *Proc. IEEE Int. Joint Conf. Biometrics*, 2011, pp. 1–7.

[54] L. Rong, Z. Jianzhong, L. Ming, and H. Xiangfeng, "A wearable acceleration sensor system for gait recognition," in *Proc. IEEE Conf. Industrial Electron. Appl.*, 2007, pp. 2654–2659.
[55] S. Sprager and D. Zazula, "A cumulant-based method for gait identification using accelerometer data with principal component analysis and support vector machine," *WSEAS Trans. Signal Process.*, vol. 5, no. 11, pp. 369–378, 2009.
[56] J. R. Kwapisz, G. M. Weiss, and S. A. Moore, "Cell phone-based biometric identification," in *Proc. 4th IEEE Int. Conf. Biometrics: Theory Appl. Syst.*, 2010, pp. 1–7.
[57] J. Frank, S. Mannor, J. Pineau, and D. Precup, "Time series analysis using geometric template matching," *IEEE Trans. Pattern Anal. Mach. Intell.*, vol. 35, no. 3, pp. 740–754, 2013.
[58] H. Sun, T. Yuan, X. Li, and Y. Hu, "Accelerometer-based gait authentication via neural network," *Chin. J. Electron.*, vol. 21, no. 3, pp. 481–484, May 2012.
[59] W. Xu, G. Revadigar, C. Luo, N. Bergmann, and W. Hu, "Walkie-talkie: Motion-assisted automatic key generation for secure on-body device communication," in *Proc. 15th ACM/IEEE Int. Conf. Inf. Process. Sensor Netw.*, 2016, pp. 1–12.
[60] D. Schürmann, A. Brüsch, S. Sigg, and L. Wolf, "Bandanabody area network device-to-device authentication using natural gait," in *Proc. IEEE Int. Conf. Pervasive Comput. Commun.*, 2017, pp. 190–196.
[61] G. Revadigar, C. Javali, W. Xu, A. V. Vasilakos, W. Hu, and S. Jha, "Accelerometer and fuzzy vault based secure group key generation and sharing protocol for smart wearables," *IEEE Trans. Inf. Forensics Security*, vol. 12, no. 10, pp. 2467–2482 Oct. 2017.
[62] S. Khalifa, G. Lan, M. Hassan, A. Seneviratne, and S. K. Das, "Harke: Human activity recognition from kinetic energy harvesting data in wearable devices," *IEEE Trans. Mobile Comput.*, Oct. 2017 (In press), doi: 10.1109/TMC.2017.2761744.
[63] G. Lan, W. Xu, S. Khalifa, M. Hassan, and W. Hu, "Transportation mode detection using kinetic energy harvesting wearables," in *Proc. IEEE Int. Conf. Pervasive Comput. Commun. Workshops*, 2016, pp. 1–4.
[64] G. Lan, W. Xu, S. Khalifa, M. Hassan, and W. Hu, "Veh-com: Demodulating vibration energy harvesting for short range communication," in *Proc. IEEE Int. Conf. Pervasive Comput. Commun.*, 2017, pp. 170–179.

**Weitao Xu** received the bachelor's of engineering and master's of engineering degrees from the School of Information Science and Engineering, Shandong University, Shandong, China, in 2010 and 2013, respectively, and the PhD degree from the University of Queensland, in 2017. He is currently a research associate with the College of Computer Science and Software Engineering, Shenzhen University, China. He is a member of the IEEE.

**Guohao Lan** received the BE degree in software engineering from the Harbin Institute of Technology, China, in 2012, and the MS degree in computer science from the Korea Advanced Institute of Science and Technology (KAIST), Korea, in 2015, He is currently working toward the PhD degree from the School of Computer Science and Engineering, the University of New South Wales, Australia. His research interests include wireless networks, pervasive computing, and energy-efficient systems.

**Qi Lin** received the bachelor's degree in automation from Zhejiang University, China, in 2007, the master's degree in mechatronics from the University of Adelaide, Australia, in 2010, and the master's degree in information technology from the University of New South Wales (UNSW), in 2016. He is currently working toward the PhD degree in the School of Computer Science and Engineering, (UNSW), Australia.

**Sara Khalifa** received the PhD degree in computer science and engineering from the University of New South Wales, Sydney, Australia. She is currently a research scientist with the Distributed Sensing Systems Research Group, Data61—CSIRO. Her research interests include internet of things, smart wearables, energy harvesting, and pattern recognition. She is the recipient of the 2017 John Makepeace Bennett Award which is awarded by CORE (Computing Research and Education Association of Australasia) to the best PhD dissertation of the year within Australia and New Zealand in the field of computer science. She is a member of the IEEE.

**Mahbub Hassan** received the MSc degree in computer science from the University of Victoria, Canada, and the PhD degree in computer science from Monash University, Australia. He is a full professor with the School of Computer Science and Engineering, the University of New South Wales, Sydney, Australia. He is a senior member of the IEEE and served as a Distinguished Lecturer of IEEE (COMSOC) for 2013-2016. He is currently an editor of the *IEEE Communications Surveys and Tutorial* and has previously served as guest editor for *IEEE Network*, *IEEE Communications Magazine*, *IEEE Transactions on Multimedia*, and area editor for *Computer Communications*. More information is available at http://www.cse.unsw.edu.au/ mahbub.

**Neil Bergmann** received the BE, BS, and BA degrees from The University of Queensland, Brisbane, Australia, and the PhD degree in computer science from the University of Edinburgh, Edinburgh, United Kingdom. He is currently a professor of embedded systems with The University of Queensland. His research interests include computer architecture, and wireless sensor networks. He is a fellow of the Institution of Engineers, Australia.

**Wen Hu** is a senior lecturer with the School of Computer Science and Engineering, the University of New South Wales (UNSW). Much of his research career has focused on the novel applications, low power communications, security and compressive sensing in sensor network systems, and Internet of Things (IoT). He is a senior member of the IEEE.